Updated phylogeny and sequence features of MreB from the wall-less bacteria *Spiroplasma*

Daichi Takahashi[a], Ikuko Fujiwara[a,b], Makoto Miyata[a,b,#]

[a]Graduate School of Science, Osaka City University, Osaka, Japan

[b]The OCU Advanced Research Institute for Natural Science and Technology (OCARINA), Osaka City University, Osaka, Japan

Running Title: Sequence analyses for *Spiroplasma* MreBs

#Address correspondence to Makoto Miyata, miyata@sci.osaka-cu.ac.jp

ABSTRACT *Spiroplasma* are bacteria with a helical cell shape and a lack of peptidoglycan. They belong to the phylum *Tenericutes* that evolved from *Firmicutes,* which includes the bacterium *Bacillus subtilis*. *Spiroplasma* swimming motility is unrelated to widespread bacterial motilities, such as flagellar motility, and is caused by helicity switching with kinks traveling along the helical cell body. The swimming force is likely generated by five classes of bacterial actin homolog MreBs involved in the helical bone structure. We analyzed sequences of *Spiroplasma* MreBs (SMreBs) to clarify their phylogeny and sequence features. The maximum likelihood method based on around 5,000 MreB sequences showed that the phylogenetic tree was divided into several radiations: MreBs of conventional bacteria, MreBs of candidate phyla radiation, and radiations for *Firmicutes* MreB isoforms. SMreBs formed a clade adjacent to the radiation of MreBH, an MreB isoform of *Firmicutes*. Sequence comparisons of SMreBs and *Bacillus* MreBs were also performed to clarify the features of SMreB. In SMreBs 2 and 4, amino acids involved in the interactions for inter- and intra-protofilament were significantly different from those in *Bacillus* MreBs. Catalytic glutamic acid and threonine were changed to aspartic acid and lysine, respectively, in SMreB3.

SMreB5 had a significantly longer C-terminal region than the other MreBs, which possibly forms a protein-protein interaction unique to *Spiroplasma*. A membrane-binding region was not identified in most SMreBs 1 and 4, although it is conserved in many walled bacterial MreBs. These features may support the functions responsible for the unique mechanism of *Spiroplasma* swimming.

IMPORTANCE *Spiroplasma*, a small bacterial group, is parasitic to plants and arthropods. *Spiroplasma* species are globally widespread and swim via a “helicity switching” mechanism. This mechanism is caused by fibril, a *Spiroplasma*-specific protein, and five classes of MreBs, bacterial actin belonging to the same family as major muscle protein. This study clarified the evolutional and structural features of MreBs and provided possible clues to control the industrial damage caused by *Spiroplasma* and develop manageable nano-devices to mimic helicity switching.

50 **INTRODUCTION**

51 The phylum *Tenericutes* consists of bacteria that evolved from the phylum
52 *Firmicutes* (1, 2). Currently, *Tenericutes* is comprised only of the class *Mollicutes*,
53 which includes the genera *Spiroplasma* and *Mycoplasma*. Species of these genera
54 are characterized by small genome size, low guanine and cytosine contents, being
55 mostly parasitic or commensal, and absence of peptidoglycan (3). In addition, they
56 cannot equip conventional machineries for bacterial motility, such as flagella or
57 type IV pili, due to the lack of a peptidoglycan layer (4). Instead, they have
58 developed three unique motility systems: *mobile* type gliding, *pneumoniae* type
59 gliding, and *Spiroplasma* swimming (4-11).

60 *Spiroplasma* have a helical cell shape and infect multi-cellular organisms, such
61 as plants and arthropods (12). They swim by rotating the cell body in viscous
62 environments, including host tissues. To rotate the cell body, *Spiroplasma* change
63 the helicity handedness at the front end by forming a kink, and propagate the kink
64 along the cell body from front to back (Fig 1A-B refer to videos in the following
65 articles) (11, 13-15). The helical cell shape originates from a flat ribbon structure
66 extending along the innermost line of the cell, and kink propagation is likely caused

67 by a structural change of the ribbon structure (Fig 1C) (13, 16-18). Electron
68 microscopy and proteome analyses have revealed that the flat ribbon is composed
69 of fibril, a *Spiroplasma* specific protein that forms a helical filament, and MreB
70 proteins, which are bacterial actin homologs (Fig 2A) (16-18). On the other hand,
71 seven copies of *mreB* genes have been found on the draft genome of a
72 *Tenericutes* bacterium, *Haloplasma contractile*, which performs characteristic
73 motility via tentacle-like structures extending from a coccoidal body (19, 20). Based
74 on these findings, MreBs are thought to be employed in the motility of *Tenericutes*
75 (16, 19). *Candidatus* Izimaplasma and *Mesoplasma* are spherical bacteria that
76 belong to *Tenericutes*. *Candidatus* Izimaplasma have three and *Mesoplasma* have
77 one *mreB* gene/s, respectively (19, 21, 22). While their motilities have not yet been
78 reported, it is possible that they use MreBs for motility.
79 As seen in eukaryotic actin, the MreB molecule has a U-shaped three
80 dimensional (3D) structure that can be further divided into four domains (Fig 2A)
81 (23, 24). The groove of the U-shaped structure functions as a nucleotide-binding
82 pocket, such as for ATP and GTP (Fig S3A) (23, 25-27). A previous study reported
83 that, in the presence of nucleotides, especially ATP, MreB polymerizes into non-

84 helical filaments with juxtaposed subunits in which two protofilaments interact
85 antiparallelly (Fig 2B) (23). Molecular dynamics (MD) simulations suggest that the
86 inter- and intra-protofilament interactions are comprised of four helices, two
87 strands, and three loops (H3, H5, and H8 shown in Fig 2A and Fig S3C for inter-
88 protofilament interaction; H9, S12, S13 and loops between S6-H1, S9-S10, and
89 S10-S11 shown in Fig 2A and Fig S3D for intra-protofilament interaction) (28).
90 Unlike the eukaryotic actin filament, MreB filaments bind to the cell membrane
91 directly (29). A previous study reported that many MreBs have two consecutive
92 hydrophobic amino acids for membrane binding in the hydrophobic loops in domain
93 IA (Fig 2A) (29). The study also reported that some MreBs of gram-negative
94 bacteria have an amphipathic helix at the N-terminus as an additional factor for
95 membrane binding (Fig 2A).
96 In various phyla of rod-shaped bacteria, MreB is well-conserved in the genomes
97 and is responsible for cell shape maintenance (30, 31). The MreB filament binds to
98 the membrane to form an elongasome complex with other proteins, which precisely
99 locates the peptidoglycan-synthesizing enzymes to retain the rod shape of the cells
100 (30, 31). Many bacterial species represented by *Escherichia coli* have a single

101 copy of the *mreB* gene on their genome (31), whereas the genome of *Bacillus*
102 *subtilis* has three genes to code MreB isoforms (MreB, Mbl, and MreBH), all of
103 which are employed in cell shape maintenance (32-35). The role of MreB is similar
104 to that of other bacterial actin homologs, such as ParM, MamK, and FtsA, which
105 are also responsible for the assignment of materials such as DNA, vesicles, and
106 cytoskeletal rings in cells (36).

107 As *Spiroplasma* MreBs (SMreBs) have a role that is distinct from those of other
108 bacterial actin homologs, sequence analyses among SMreBs and walled-bacterial
109 MreBs are useful for clarifying the origin and mechanism of *Spiroplasma*
110 swimming. While a previous study reported that *Spiroplasma* and *Haloplasma* form
111 two independent phylogenetic groups, the phylogenetical relationship among
112 SMreBs and walled-bacterial MreBs remains unclear (19). Moreover, amino acid
113 sequences specific for MreB functions, including nucleotide binding and hydrolysis,
114 interaction regions to form double-stranded filaments, and membrane binding
115 regions, have not yet been characterized for SMreBs.

116 In this study, we analyzed the sequences of SMreBs. Phylogenetic analyses
117 suggested that SMreBs evolved from MreBH in *Firmicutes*. Sequence comparisons

118 of SMreBs and *Bacillus* MreBs clarified their sequence features for ATP hydrolysis,

119 interactions for filament formation, and membrane binding.

120

121 **RESULTS AND DISCUSSION**

122 **Evolutional relationships between *Spiroplasma* and other MreBs**

123 We analyzed the phylogenetic relationships among SMreBs and other MreBs.

124 We first obtained 5,002 amino acid sequences of MreB family proteins through a

125 BLAST search, including all 170 non-redundant sequences of SMreB with those of

126 three new species (*S*. sp. TU-14, *S*. sp. ChiS and *S*. endosymbiont of *Megaselia*

127 *nigra*) (Table S1) (Data set 1) (37-40). Based on these sequences, we constructed

128 a maximum likelihood phylogenetic tree (Fig 3, S7). We adopted this phylogenetic

129 tree because the topology difference was indistinguishable between 4,000 and

130 5,002 sequences. The largest radiation of the phylogenetic tree consisted of MreB

131 family proteins of conventional bacteria, including *Bacillus* MreBs (BMreB). Similar

132 to the phylogenetic tree based on ribosomal proteins (1, 2), the radiation was

133 further divided into gram-positive bacteria, which have an outer membrane, and

134 gram-negative bacteria, which do not. Previous studies of MreB family proteins

135 have primarily focused on proteins in these radiations (31), unlike the present
136 study. In our phylogenetic tree, an MreB radiation of candidate phyla radiation
137 (CPR) (1, 2) (also known as Patescibacteria (41)) was formed next to the MreB
138 radiation of conventional bacteria. The CPR MreBs were split into two clades. Four
139 CPR candidate species in candidate phyla Yanofskybacteria, Taylorbacteria,
140 Zambryskibacteria, and Woesebacteria had MreBs of both clades, suggesting that
141 there are two types of MreBs that possess different roles in CPR.
142 *Firmicutes* bacteria have more than one copy of a gene to code MreB isoforms
143 on the genomes (32), forming three clades of MreB isoforms in addition to the
144 MreB radiations mentioned above. One was mostly composed of class *Bacilli* MreB
145 family proteins related to *Bacillus* Mbl. Another clade positioned between clades of
146 *Bacillus* Mbl and CPR MreB was primarily composed of proteins in class *Clostridia*,
147 distantly related to *Bacillus* MreB isoforms, suggesting the existence of a new
148 group of MreB isoforms. The clade including *Bacillus* MreBH (BMreBH) had a root
149 distinct from other clades. SMreBs formed a radiation near the BMreBH clade. In
150 addition, a clade of MreBs from *Haloplasma* and Izimaplasma species (HMreB)
151 was identified between clades of SMreB and BMreBH (Fig 3, S1). These

152 relationships suggest that the MreBs of *Tenericutes* species, SMreB and HMreB,
153 evolved from BMreBH.
154
155 **Development of *Spiroplasma* swimming**
156 Based on the phylogeny results and presence of genes for MreB isoforms in
157 each bacterium, we assessed the evolutional background prior to *Spiroplasma*
158 acquiring swimming motility using a phylogenetic tree of 16S rRNA, including newly
159 obtained *Spiroplasma* species (Fig 4, Data set 2) (37-40). A *Firmicutes* species, the
160 putative ancestor of *Tenericutes*, probably possessed MreB, Mbl, and MreBH as
161 the *Firmicutes* species closest to *Tenericutes* had these three MreB isoforms, as
162 reported previously (1, 2). The ancestral bacterium then likely lost MreB and Mbl
163 and duplicated MreBH before *Haloplasma* and other *Tenericutes* bacteria
164 separated. After the duplication of MreBH, *Haloplasma* and Izimaplasma likely
165 acquired HMreBs. HMreB may be involved in the characteristic motility of
166 *Haloplasma* (20), while that in Izimaplasma is unknown because its motility has not
167 yet been reported. A previous study suggested that *Haloplasma* and *Spiroplasma*
168 acquired their MreBs by independent gene duplications (19). However, HMreB was

169 located closer to SMreB and MreBH than to the other clades in our phylogenetic
170 tree (Fig 3, S1). Therefore, *Spiroplasma* likely acquired SMreBs by the duplication
171 of MreBH, as suggested in *Haloplasma* and Izimaplasma (Fig 4). Fibril, another
172 component of the ribbon structure of *Spiroplasma* cells, is specific for *Spiroplasma*
173 (Fig 1C) (11, 16, 17, 19, 42). Therefore, fibril was likely acquired after *Spiroplasma*
174 and Izimaplasma separated and may function with SMreBs to allow *Spiroplasma*
175 swimming.

176 The *Spiroplasma* genus can be divided into two subgroups: Apis and Citri-
177 Chrysopicola-Mirum (Citri) (19, 37-39). In terms of the *Spiroplasma* genomes,
178 duplications of SMreBs 1, 4, or 5 and deletions of SMreBs 1 or 2 were identified in
179 almost all species of the Apis group, unlike the Citri group, as previously reported
180 (19). *Spiroplasma* swimming has been studied by using Citri species (*S. melliferum*
181 and *S. eriocheiris*), both of which swim via similar kink propagations (11, 15-18,
182 42). The duplication and deletion of SMreBs in the Apis group may suggest their
183 diverse swimming formats.

184

185 **Sequence comparisons among SMreBs and BMreBs**

186 We compared the amino acid sequences of SMreB, HMreB, BMreB, and
187 BMreBH to characterize SMreBs (Fig 2C, S6). First, the conserved amino acids of
188 SMreBs 1-5, HMreB, and BMreBH sequences were compared with those of 48
189 sequences of BMreBs (Fig 2C, S6). Each SMreB type showed specific conserved
190 sequences different from those of BMreBs. SMreB 1-5 conserved 128, 187, 46,
191 210, and 121 amino acids in approximately 330 full-length amino acid sequences,
192 respectively. Of these amino acids, 50, 102, 21, 122, and 53 amino acids were
193 specific for each SMreB, respectively, and were not conserved in BMreBs (Table
194 S2, Fig 2C, S6). The specificity of these sequences to SMreBs suggests the
195 importance of the sequences for functions unique to SMreBs. Sequences of Citri
196 group SMreBs were more conserved than those of the Apis group, corresponding
197 to the phylogenetical spread among *Spiroplasma* species represented in the 16S
198 rRNA phylogeny (Table S3-4, Fig 4, S2, S6).
199

200 **Characterization of SMreBs based on amino acid sequences**

201 Next, to investigate the SMreB sequences corresponding to the sequences
202 conserved in walled bacteria (23, 28, 29, 43, 44), we predicted the ancestral

203 sequences and 3D structures for SMreBs 1-5, HMreB, BMreBH, and BMreB (Fig
204 S2, Data set 3). First, we focused on the 19 amino acids that construct the
205 nucleotide binding pocket (Fig 2A, D, S3A) (44) because MreB polymerization is
206 initiated when a nucleotide, such as ATP or GTP, binds to this pocket. In SMreB
207 sequences, most of the 12 amino acids conserved in BMreBH were also
208 conserved, except E212 (Fig 2C black dashed line boxes, Fig 2D, S6). We also
209 focused on the catalytic amino acids for nucleotide hydrolysis (23). While a
210 glutamic acid and threonine were conserved in almost all MreBs, interestingly, in
211 SMreB3, these sequences were changed to an aspartic acid and lysine,
212 respectively (Fig 2C cyan solid line boxes, Fig 2D, S6). As mutations on the
213 catalytic amino acids reduce depolymerization rates of eukaryotic actin and MamK
214 (45, 46), SMreB3 may also have different polymerization or depolymerization rates
215 than other SMreBs. Generally, an antibiotic A22 inhibits MreB polymerization by
216 interacting with the nucleotide in the MreB molecule (43). SMreBs also conserved
217 these target amino acids of A22, which was predicted by MD simulations based on
218 the crystal structure (Fig 2A, S3B, Fig 2C red dashed line boxes, Fig S6) (43).
219 Next, we focused on 87 amino acids involved in the inter- and intra-protofilament

220 interactions (H3, H5, H8, H9, S12, and S13 and loops between S6-H1, S9-S10,
221 and S10-S11 in Fig 2A, Fig S3C-D) (28). In these regions, 31, 50, 14, 69, and 32
222 amino acids were conserved in SMreBs 1-5, respectively (Fig 2C light green and
223 cyan dashed line boxes, Fig 2E-F, S6). In these amino acids, 15, 26, 6, 40, and 16
224 sequences were not conserved in BMreBs, respectively (white characters in light
225 green and cyan dashed line boxes in Fig 2C). As these regions in a walled-
226 bacterial MreB move toward an adjacent MreB molecule to interact with each other
227 (28), these amino acid substitutions of SMreBs, especially SMreBs 2 and 4, may
228 affect the flexibility and interaction strength of these regions, allowing them to show
229 polymerization characteristics different to those of walled-bacterial MreB.
230 We also characterized regions required for membrane binding. Two consecutive
231 hydrophobic amino acids are conserved in many walled-bacterial MreBs (Fig 2A).
232 However, SMreBs 1 and 4 of the Citri group did not have hydrophobic amino acids
233 (Fig 2C red solid line box, Fig S6) (23, 29). Moreover, the hydrophobic amino acids
234 cannot be found in 46 out of 88 sequences of the Apis group SMreBs 1, 3, 4, and 5
235 (Fig S6). These SMreBs may not directly interact with the membrane. All other
236 SMreBs (Apis group SMreB2 and Citri group SMreBs 2, 3, and 5) had hydrophobic

237 amino acids (Fig 2C, S6). We next focused on the N-terminal amphipathic helix
238 found in some MreBs of gram-negative bacteria (Fig 2A). All N-terminal regions of
239 the Citri group SMreB3, except for *S. melliferum* strain AS576 (QCO24517.1), were
240 predicted to take amphipathic helices (Fig 2C light green solid line, Fig S4A-F).
241 Interestingly all SpeMreB3 possessed a threonine at the hydrophobic sides (Fig
242 S4G, S6). This suggests that Citri group SMreB3 proteins also have affinity to the
243 membrane through the helix.
244 The lengths of C-terminal sequences varied among 133 SMreBs, and over 79%
245 of SMreBs were eight amino acids longer than that of BMreB (Fig S5, S6, Table
246 S5). In particular, SMreB5 had the longest C-terminal sequence of all SMreBs
247 (Table S5). Such terminal extension is a feature reminiscent of a bacterial tubulin
248 homolog, FtsZ, featured with a long unstructured region known as C-terminal
249 Conserved Peptide (CCP) (47). This is the interaction region for several proteins,
250 including FtsA, ZipA, and ZapD, involved in Z-ring formation, which causes cell
251 constriction for bacterial cytokinesis (47-50). The extension of the SMreB C-termini
252 may play a role in the protein-protein interactions of *Spiroplasma*, as observed in
253 FtsZ.

254

255 ## CONCLUSIONS

256 In this study, we suggested that the five classes of SMreBs evolved from MreBH
257 (Fig 3) and clarified that the classes can be characterized by polymerization,
258 membrane binding, and protein interactions. Based on these results, we suggest
259 the functions for individual SMreBs. SMreBs 2, 3, and 4 may form filaments of
260 sufficient size to be observed via electron microscopy, as reported previously (Fig
261 2C-F, S6) (17, 18). Citri group SMreBs 2, 3, and 5 can bind to membranes, but Citri
262 group SMreBs 1 and 4 cannot (Fig 2C, S6). SMreB5 may interact with other
263 proteins, such as fibril protein via their C-terminal regions (Fig 2C, Table S5, S6).
264 These findings would allow the clarification of the origin and mechanism of
265 *Spiroplasma* swimming.

266

267 ## MATERIALS AND METHODS

268 **Phylogenetical analyses**

269 A protein BLAST search on non-redundant protein sequences was performed to
270 collect 5,000 amino acid sequences of MreB in ascending order of E value by

271 templating MreB3 of *S. eriocheiris* (NCBI accession: WP_047791951.1) on July 14,
272 2019. Sequences of *B. subtilis* MreB isoforms annotated to MreB (AQR87043.1)
273 and MreBH (BAA07047.1) were added to the 5,000 sequences as representative
274 sequences, although the closest sequences were identified by the BLAST search
275 (WP_039074652.1; 99.11% identical with AQR87043.1, WP_061522102.1; 95.52%
276 identical with BAA07047.1). The nucleotide sequences of 16S rRNA were identified
277 by independent searches in the GenBank database. The sequence alignments and
278 construction of phylogenetic trees were performed via the MUSCLE program and
279 maximum likelihood method, respectively, using MEGA-X ver. 10.1 (51). Bootstrap
280 supports were estimated from 100 samples of alignment. To estimate the ancestor
281 of MreBs in each group, maximum likelihood phylogenetic trees by each MreB
282 group were constructed with a *B. subtilis* MreB (an *E. coli* MreB for the ancestor
283 estimation of *Bacillus* MreB) as an outgroup, and the ancestral sequences were
284 estimated by the ancestor estimation program of MEGA-X ver. 10.1 (51).
285

286 **Structure prediction and sequence analyses**

287 All monomeric MreB structures in this study were predicted using Rosetta

288 comparative modeling by templating a structure of *Caulobacter crescentus* MreB
289 (PDB ID: 4CZJ), using Robetta software (23, 52). Sequence comparisons among
290 *Spiroplasma*, *Haloplasma*, Izimaplasma, and *Bacillus* MreB isoforms were
291 performed by Clustal Omega (53). Duplicated SMreBs 1, 4, and 5 in the Apis group
292 species were incorporated into the analyses. Seven of the 19 amino acid
293 sequences contained in SMreB3 of the Apis group had no annotation. Since these
294 proteins were coded in a position suggesting SMreB3 as an ortholog on the
295 genome, they were included in the analyses. SMreB3 of the *S. melliferum* strain
296 CH-1 (NCBI accession: AHA83319.1) was excluded from the analyses because it
297 was approximately 130 amino acids shorter than the other SMreB3 sequences
298 comprising approximately 330 amino acids. Two sequences, MreB4 of *S.*
299 *eriocheiris* strain CCTCC_M_207170 (AHF58342.1) and a protein from *S.*
300 *culicicola*, which is unannotated but can be classified to MreB3
301 (WP_025363622.1), were not used for the analyses because the initiation codon
302 was miss-assigned. The predictions of secondary structures and amphipathic
303 helices were performed using PSIPRED 4.0 and AmphipaSeeK software,
304 respectively (54-56). Sequence identity and similarity were calculated as the ratio

305 of amino acids with identity and strong similarity defined by the Gonnet PAM 250

306 matrix over the total amino acid number excluding gap regions.

307

308 **ACKNOWLEDGEMENTS**

309 We thank Yuya Sasajima and Hana Kiyama at the Graduate School of Science,

310 Osaka City University, Japan for helpful discussion. The electron microscope

311 image of *Spiroplasma* (Fig 1A) and the schematic image of the ribbon structure

312 (Fig 1C) were courtesy of Yuya Sasajima (Osaka City University, Japan). This

313 study was supported by a Grants-in-Aid for Scientific Research (A and C) (MEXT

314 KAKENHI, Grant Numbers JP17H01544 to MM and JP20K06591 to IF), JST

315 CREST (Grant Number JPMJCR19S5) to MM, Research Foundation of Opto-

316 Science and Technology to IF, and the Osaka City University (OCU) Strategic

317 Research Grant 2019 to IF. DT is a recipient of a Japanese scholarship of JEES

318 Kureha (Toyobo) Scholarship.

319

320 **REFERENCES**

321 1. Castelle CJ, Banfield JF. 2018. Major new microbial groups expand diversity

322 and alter our understanding of the tree of life. Cell 172:1181-1197.

323 2. Hug LA, Baker BJ, Anantharaman K, Brown CT, Probst AJ, Castelle CJ,
324 Butterfield CN, Hernsdorf AW, Amano Y, Ise K, Suzuki Y, Dudek N, Relman
325 DA, Finstad KM, Amundson R, Thomas BC, Banfield JF. 2016. A new view
326 of the tree of life. Nat Microbiol 1:16048.

327 3. Razin S, Hayflick L. 2010. Highlights of mycoplasma research--an historical
328 perspective. Biologicals 38:183-90.

329 4. Miyata M, Robinson RC, Uyeda TQP, Fukumori Y, Fukushima S, Haruta S,
330 Homma M, Inaba K, Ito M, Kaito C, Kato K, Kenri T, Kinosita Y, Kojima S,
331 Minamino T, Mori H, Nakamura S, Nakane D, Nakayama K, Nishiyama M,
332 Shibata S, Shimabukuro K, Tamakoshi M, Taoka A, Tashiro Y, Tulum I, Wada
333 H, Wakabayashi K. 2020. Tree of motility - A proposed history of motility
334 systems in the tree of life. Genes to Cells 25:6-21.

335 5. Nishikawa MS, Nakane D, Toyonaga T, Kawamoto A, Kato T, Namba K,
336 Miyata M. 2019. Refined mechanism of *Mycoplasma mobile* gliding based
337 on structure, ATPase activity, and sialic acid binding of machinery. mBio
338 10:e02846-19.

339 6. Mizutani M, Miyata M. 2019. Behaviors and energy source of *Mycoplasma*
340 *gallisepticum* gliding. J Bacteriol 201:e00397-19.
341 7. Mizutani M, Tulum I, Kinosita Y, Nishizaka T, Miyata M. 2018. Detailed
342 analyses of stall force generation in *Mycoplasma mobile* gliding. Biophys J
343 114:1411-1419.
344 8. Kinosita Y, Miyata M, Nishizaka T. 2018. Linear motor driven-rotary motion
345 of a membrane-permeabilized ghost in *Mycoplasma mobile*. Sci Rep
346 8:11513.
347 9. Miyata M, Hamaguchi T. 2016. Prospects for the gliding mechanism of
348 *Mycoplasma mobile*. Curr Opin Microbiol 29:15-21.
349 10. Miyata M, Hamaguchi T. 2016. Integrated information and prospects for
350 gliding mechanism of the pathogenic bacterium *Mycoplasma pneumoniae*.
351 Front Microbiol 7:960.
352 11. Shaevitz JW, Lee JY, Fletcher DA. 2005. *Spiroplasma* swim by a processive
353 change in body helicity. Cell 122:941-5.
354 12. Lo WS, Huang YY, Kuo CH. 2016. Winding paths to simplicity: genome
355 evolution in facultative insect symbionts. FEMS Microbiol Rev 40:855-874.

356 13. Nakane D, Ito T, Nishizaka T. 2020. Coexistence of two chiral helices
357 produces kink translation in *Spiroplasma* swimming. J Bacteriol 202:e00735-
358 19.
359 14. Terahara N, Tulum I, Miyata M. 2017. Transformation of crustacean
360 pathogenic bacterium *Spiroplasma eriocheiris* and expression of yellow
361 fluorescent protein. Biochem Biophys Res Commun 487:488-493.
362 15. Wada H, Netz RR. 2009. Hydrodynamics of helical-shaped bacterial motility.
363 Phys Rev E 80:021921.
364 16. Liu P, Zheng H, Meng Q, Terahara N, Gu W, Wang S, Zhao G, Nakane D,
365 Wang W, Miyata M. 2017. Chemotaxis without conventional two-component
366 system, based on cell polarity and aerobic conditions in helicity-switching
367 swimming of *Spiroplasma eriocheiris*. Front Microbiol 8:58.
368 17. Trachtenberg S, Dorward LM, Speransky VV, Jaffe H, Andrews SB,
369 Leapman RD. 2008. Structure of the cytoskeleton of *Spiroplasma melliferum*
370 BC3 and its interactions with the cell membrane. J Mol Biol 378:778-89.
371 18. Kurner J, Frangakis AS, Baumeister W. 2005. Cryo-electron tomography
372 reveals the cytoskeletal structure of *Spiroplasma melliferum*. Science

373 307:436-8.

374 19. Ku C, Lo WS, Kuo CH. 2014. Molecular evolution of the actin-like MreB
375 protein gene family in wall-less bacteria. Biochem Biophys Res Commun
376 446:927-32.

377 20. Antunes A, Alam I, El Dorry H, Siam R, Robertson A, Bajic VB, Stingl U.
378 2011. Genome sequence of *Haloplasma contractile*, an unusual contractile
379 bacterium from a deep-sea anoxic brine lake. J Bacteriol 193:4551-2.

380 21. Skennerton CT, Haroon MF, Briegel A, Shi J, Jensen GJ, Tyson GW, Orphan
381 VJ. 2016. Phylogenomic analysis of *Candidatus* 'Izimaplasma' species: free-
382 living representatives from a *Tenericutes* clade found in methane seeps.
383 ISME J 10:2679-2692.

384 22. Tully JG, Whitcomb RF, Hackett KJ, Rose DL, Henegar RB, Bove JM, Carle
385 P, Williamson DL, Clark TB. 1994. Taxonomic descriptions of 8 new non-
386 sterol-requiring *Mollicutes* assigned to the genus *Mesoplasma*. Int J Syst
387 Bacteriol 44:685-693.

388 23. van den Ent F, Izore T, Bharat TA, Johnson CM, Löwe J. 2014. Bacterial
389 actin MreB forms antiparallel double filaments. eLife 3:e02634.

390 24. van den Ent F, Amos LA, Löwe J. 2001. Prokaryotic origin of the actin
391 cytoskeleton. Nature 413:39-44.
392 25. Nurse P, Marians KJ. 2013. Purification and characterization of *Escherichia*
393 *coli* MreB protein. J Biol Chem 288:3469-3475.
394 26. Mayer JA, Amann KJ. 2009. Assembly properties of the *Bacillus subtilis*
395 actin, MreB. Cell Motility and the Cytoskeleton 66:109-118.
396 27. Bean GJ, Amann KJ. 2008. Polymerization properties of the *Thermotoga*
397 *maritima* actin MreB: Roles of temperature, nucleotides, and ions.
398 Biochemistry 47:826-835.
399 28. Awuni E, Mu Y. 2019. Effect of A22 on the conformation of bacterial actin
400 MreB. Int J Mol Sci 20:E1304.
401 29. Salje J, van den Ent F, de Boer P, Löwe J. 2011. Direct membrane binding
402 by bacterial actin MreB. Mol Cell 43:478-87.
403 30. Yulo PRJ, Hendrickson HL. 2019. The evolution of spherical cell shape;
404 progress and perspective. Biochem Soc Trans 47:1621-1634.
405 31. Shi H, Bratton BP, Gitai Z, Huang KC. 2018. How to build a bacterial cell:
406 MreB as the foreman of *E. coli* construction. Cell 172:1294-1305.

407 32. Schirner K, Errington J. 2009. Influence of heterologous MreB proteins on
408 cell morphology of *Bacillus subtilis*. Microbiology 155:3611-21.
409 33. Kawai Y, Asai K, Errington J. 2009. Partial functional redundancy of MreB
410 isoforms, MreB, Mbl and MreBH, in cell morphogenesis of *Bacillus subtilis*.
411 Mol Microbiol 73:719-31.
412 34. Carballido-Lopez R, Formstone A, Li Y, Ehrlich SD, Noirot P, Errington J.
413 2006. Actin homolog MreBH governs cell morphogenesis by localization of
414 the cell wall hydrolase LytE. Dev Cell 11:399-409.
415 35. Jones LJ, Carballido-Lopez R, Errington J. 2001. Control of cell shape in
416 bacteria: helical, actin-like filaments in *Bacillus subtilis*. Cell 104:913-22.
417 36. Wagstaff J, Löwe J. 2018. Prokaryotic cytoskeletons: protein filaments
418 organizing small cells. Nat Rev Microbiol 16:187-201.
419 37. Ballinger MJ, Perlman SJ. 2019. The defensive *Spiroplasma*. Curr Opin
420 Insect Sci 32:36-41.
421 38. Tsai YM, Chang A, Kuo CH. 2018. Horizontal gene acquisitions contributed
422 to genome expansion in insect-symbiotic *Spiroplasma clarkii*. Genome Biol
423 Evol 10:1526-1532.

424 39. Paredes JC, Herren JK, Schupfer F, Marin R, Claverol S, Kuo CH, Lemaitre
425 B, Beven L. 2015. Genome sequence of the *Drosophila melanogaster* male-
426 killing *Spiroplasma* strain MSRO endosymbiont. mBio 6:e02437-14.
427 40. Gasparich GE. 2002. Spiroplasmas: evolution, adaptation and diversity.
428 Front Biosci 7:d619-40.
429 41. Rinke C, Schwientek P, Sczyrba A, Ivanova NN, Anderson IJ, Cheng JF,
430 Darling A, Malfatti S, Swan BK, Gies EA, Dodsworth JA, Hedlund BP,
431 Tsiamis G, Sievert SM, Liu WT, Eisen JA, Hallam SJ, Kyrpides NC,
432 Stepanauskas R, Rubin EM, Hugenholtz P, Woyke T. 2013. Insights into the
433 phylogeny and coding potential of microbial dark matter. Nature 499:431-7.
434 42. Cohen-Krausz S, Cabahug PC, Trachtenberg S. 2011. The monomeric,
435 tetrameric, and fibrillar organization of Fib: the dynamic building block of the
436 bacterial linear motor of *Spiroplasma melliferum* BC3. J Mol Biol 410:194-
437 213.
438 43. Awuni Y, Jiang S, Robinson RC, Mu Y. 2016. Exploring the A22-bacterial
439 actin MreB interaction through molecular dynamics simulations. J Phys
440 Chem B 120:9867-74.

441 44. Aylett CH, Löwe J, Amos LA. 2011. New insights into the mechanisms of
442 cytomotive actin and tubulin filaments. Int Rev Cell Mol Biol 292:1-71.
443 45. Ozyamak E, Kollman J, Agard DA, Komeili A. 2013. The bacterial actin
444 MamK: in vitro assembly behavior and filament architecture. J Biol Chem
445 288:4265-77.
446 46. Iwasa M, Maeda K, Narita A, Maeda Y, Oda T. 2008. Dual roles of Gln(137)
447 of actin revealed by recombinant human cardiac muscle alpha-actin
448 mutants. J Biol Chem 283:21045-21053.
449 47. Gardner KA, Moore DA, Erickson HP. 2013. The C-terminal linker of
450 *Escherichia coli* FtsZ functions as an intrinsically disordered peptide. Mol
451 Microbiol 89:264-75.
452 48. Wang MZ, Fang C, Ma B, Luo XX, Hou Z. 2020. Regulation of cytokinesis:
453 FtsZ and its accessory proteins. Curr Genet 66:43-49.
454 49. Huang KH, Mychack A, Tchorzewski L, Janakiraman A. 2016.
455 Characterization of the FtsZ C-Terminal variable (CTV) region in Z-Ring
456 assembly and interaction with the Z-Ring stabilizer ZapD in *E. coli*
457 cytokinesis. PLoS ONE 11:e0153337.

458 50. Erickson HP, Anderson DE, Osawa M. 2010. FtsZ in bacterial cytokinesis:
459 cytoskeleton and force generator all in one. Microbiol Mol Biol Rev 74:504-
460 28.
461 51. Kumar S, Stecher G, Li M, Knyaz C, Tamura K. 2018. MEGA X: Molecular
462 evolutionary genetics analysis across computing platforms. Mol Biol Evol
463 35:1547-1549.
464 52. Song Y, DiMaio F, Wang RY, Kim D, Miles C, Brunette T, Thompson J, Baker
465 D. 2013. High-resolution comparative modeling with RosettaCM. Structure
466 21:1735-42.
467 53. Sievers F, Wilm A, Dineen D, Gibson TJ, Karplus K, Li W, Lopez R,
468 McWilliam H, Remmert M, Soding J, Thompson JD, Higgins DG. 2011. Fast,
469 scalable generation of high-quality protein multiple sequence alignments
470 using Clustal Omega. Mol Syst Biol 7:539.
471 54. Buchan DWA, Jones DT. 2019. The PSIPRED protein analysis workbench:
472 20 years on. Nucleic Acids Res 47:W402-W407.
473 55. Sapay N, Guermeur Y, Deleage G. 2006. Prediction of amphipathic in-plane
474 membrane anchors in monotopic proteins using a SVM classifier. BMC

475 Bioinformatics 7:255.

476 56. Jones DT. 1999. Protein secondary structure prediction based on position-

477 specific scoring matrices. J Mol Biol 292:195-202.

478

479

480 **FIGURE LEGENDS**

481 **Fig 1** *Spiroplasma* swimming. (A) Electron microscope image of *Spiroplasma*.
482 Swimming directions are indicated with yellow arrows. (B) Swimming scheme.
483 *Spiroplasma* swim via the rotation of the cell body caused by kink propagation
484 along the cell axis from front to back, which causes helicity shifts of right to left
485 (open triangle) and left to right (closed triangle). (C) Schematic image of the ribbon
486 structure responsible for swimming motility. The structure composed of SMreBs
487 and fibril protein is presented as a gold ribbon in a cell.

488

489 **Fig 2** Sequence analyses of SMreBs. (A) Structure of *Bacillus subtilis* MreB
490 predicted from the amino acid sequence (NP_390681.2). The structure is
491 composed of 15 strands and 13 helices shown as S1-S15 and H1-H13,
492 respectively. Individual subdomains are colored blue (IA), yellow (IB), red (IIA), and
493 green (IIB). An N-terminal amphipathic helix carried by some gram-negative
494 bacterial MreBs is presented as a rectangle bi-colored in blue and yellow. The
495 nucleotide binding pocket, catalytic region for nucleotide hydrolysis, A22 binding
496 region, inter- and intra-protofilament interaction regions, hydrophobic loop,

497 membrane binding amino acids in the hydrophobic loop, and N-terminal
498 amphipathic helix are marked with a rectangle common in style to those in Fig 2C.
499 (B) Filamentous structure of MreB extracted from a crystal structure of *Caulobacter*
500 *crescentus* (PDB ID: 4CZJ). It forms a non-helical filament with the juxtaposed
501 subunits in which two protofilaments interact antiparallelly. (C) Multiple alignment of
502 SMreBs 1-5, HMreB, BMreB, and BMreBH performed for MreBs 1-5 of *S.*
503 *eriocheiris*, KQ51_00688 in Izimaplasma sp. HR1, *B. subtilis* MreB, and *B. subtilis*
504 MreBH. The conservation levels for amino acids calculated from multiple
505 alignments of each MreB are indicated by the color gradient of orange markers
506 (amino acids calculated as identical, strongly conserved, and weakly conserved
507 based on the Gonnet PAM 250 matrix are indicated by deep, medium, and light
508 orange markers, respectively. Unrelated amino acids based on the matrix are not
509 colored by makers). In SMreBs 1-5, HMreB, and BMreBH, the conserved amino
510 acids, whose corresponding amino acids in BMreB were conserved as a different
511 amino acid or were not conserved, are indicated by white characters. Domains IA,
512 IB, IIA, and IIB are identified by underbars of coordinated colors with panel (A).
513 Sequences important for the specific function of MreB are indicated by rectangles

514 with different styles. (D-F) Focused amino acids are shown as 3D structures. The
515 structures for SMreBs 1-5, BMreB, HMreB, and BMreBH were marked as 1-5, B,
516 HI, and BH, respectively. The amino acids were colored red, pink, blue, or gold,
517 based on the conservation levels compared to BMreBs (red: conserved amino
518 acids whose corresponding amino acids in BMreB were conserved as different
519 amino acids, pink: conserved amino acids whose corresponding amino acids in
520 BMreB were not conserved, blue: not conserved amino acids whose corresponding
521 amino acids in BMreB were conserved, gold: conserved amino acids whose
522 corresponding amino acids in BMreB were conserved as the same amino acid).
523 The number of helices and strands is indicated for colored parts. (D) Nucleotide
524 binding pocket. The backbone atoms of catalytic amino acids for nucleotide
525 hydrolysis are indicated by spheres. (E) Inter-protofilament interaction region. (F)
526 Intra-protofilament interaction region.
527
528 **Fig 3** No rooted maximum likelihood phylogenic tree for 5,002 amino acid
529 sequences of MreB family proteins. Each clade is colored according to the major
530 phyla (or classes). Major and minor taxa in each clade are indicated without and

531 with parentheses, respectively. The branches of MreB isoforms in *Bacillus subtilis*

532 are marked by red circles. The scale bar is in units of the number of amino acid

533 substitutions per site.

534

535 **Fig 4** Maximum likelihood phylogeny for 16S rRNA of the organisms that are

536 related to the evolution of *Spiroplasma*. Sequences for 16S rRNA of proteobacteria

537 (*E. coli*, *Caulobacter vibrioides*, and *Helicobacter pylori*) were used as the

538 outgroup. Bootstrap support values are indicated by circles on nodes, solid circles

539 for support of 89% and above, and open circles for 60% to 89%. Stars and

540 triangles marked for each species indicate one duplication and deletion for genes

541 of MreBs colored differently as yellow: SMreB1, green: SMreB2, black: SMreB4,

542 and red: SMreB5. The scale bar is in units of the number of amino acid

543 substitutions per site.

Figure 1

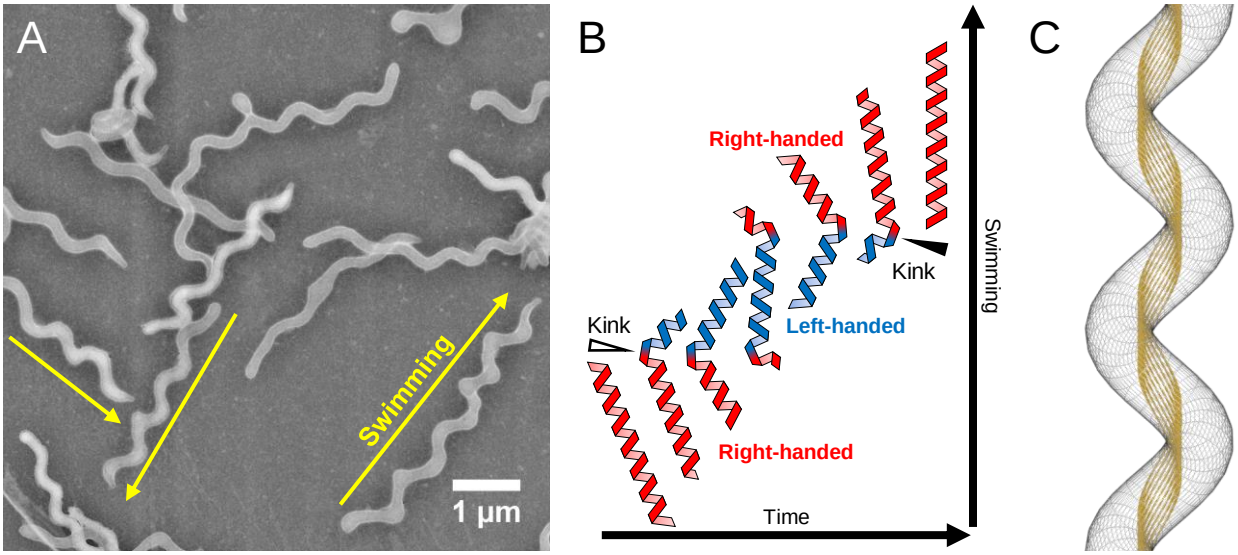
A
Swimming
1 µm
B
Right-handed
Kink
Left-handed
Kink
Right-handed
Time
Swimming
C

Figure 2

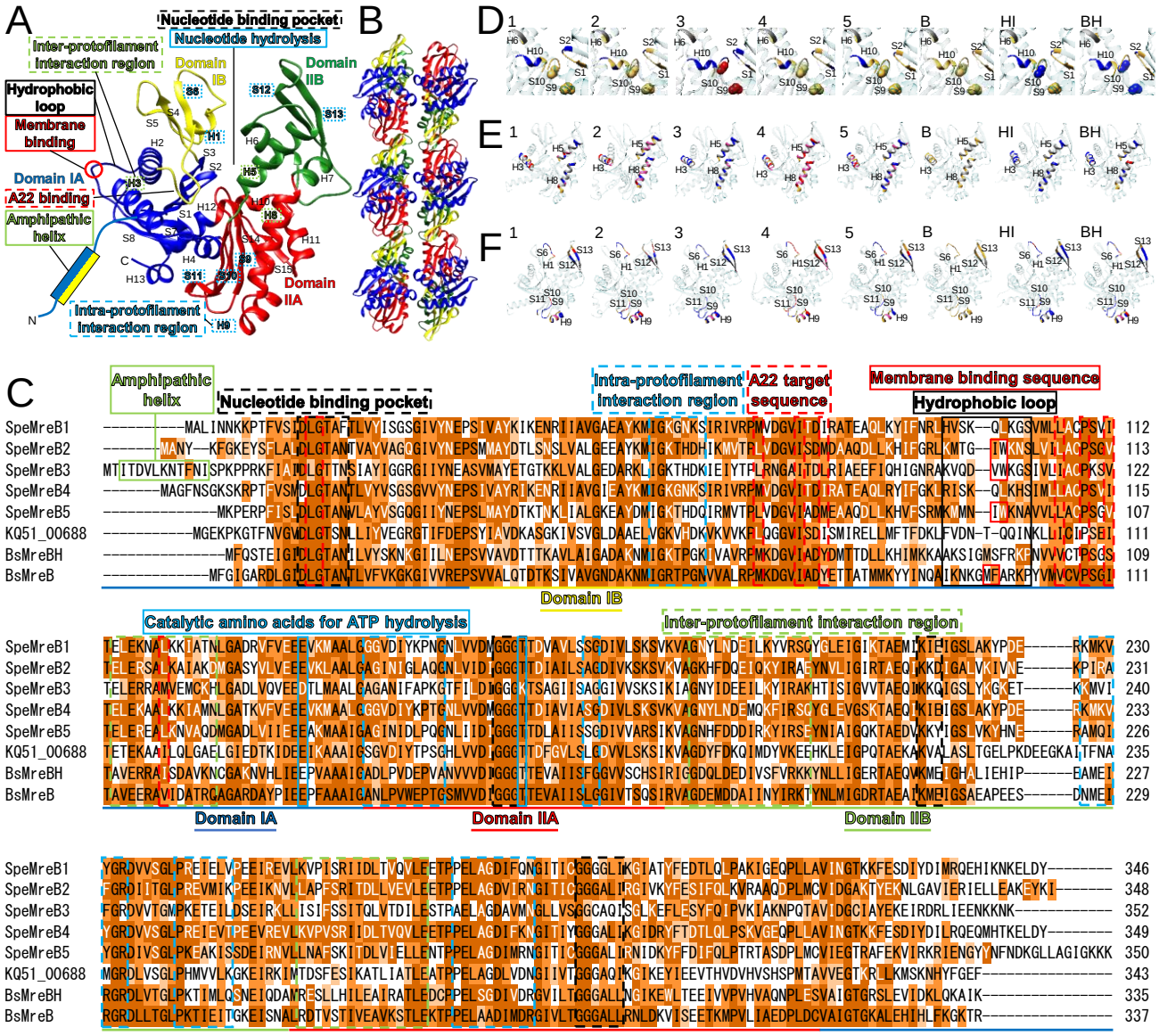
A
Nucleotide binding pocket
Nucleotide hydrolysis
Inter-protofilament interaction region
Domain IB
Domain IIB
Hydrophobic loop
Membrane binding
Domain IA
A22 binding
Amphipathic helix
Domain IIA
Intra-protofilament interaction region
B
D
E
F
C
Amphipathic helix
Nucleotide binding pocket
Intra-protofilament interaction region
A22 target sequence
Membrane binding sequence
Hydrophobic loop
Domain IB
Catalytic amino acids for ATP hydrolysis
Inter-protofilament interaction region
Domain IA
Domain IIA
Domain IIB
SpeMreB1
SpeMreB2
SpeMreB3
SpeMreB4
SpeMreB5
KQ51_00688
BsMreBH
BsMreB
Conservation level

Figure 3

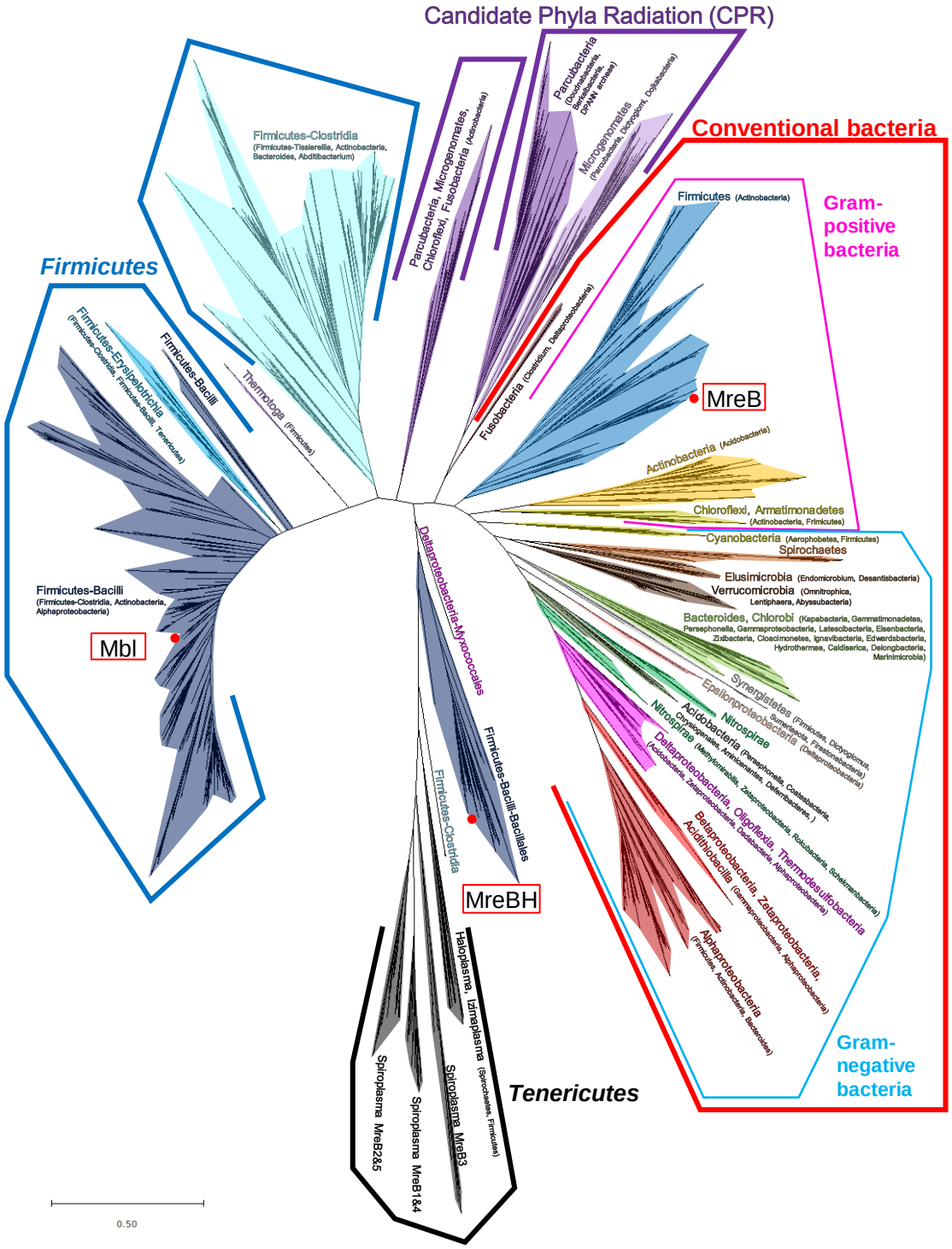
Candidate Phyla Radiation (CPR)
Conventional bacteria
Gram-positive bacteria
Gram-negative bacteria
Firmicutes
Tenericutes
Firmicutes-Clostridia
(Firmicutes-Tissierellia, Actinobacteria, Bacteroides, Abditibacterium)
Parcubacteria, Microgenomates, Chloroflexi, Fusobacteria (Actinobacteria)
Parcubacteria
(Gracilibacteria, Saccharibacteria, DPANN archaea)
Microgenomates
(Parcubacteria, Dictyoglomi, Dojkabacteria)
Firmicutes (Actinobacteria)
Fusobacteria (Clostridium, Deltaproteobacteria)
Firmicutes-Erysipelotrichia
(Firmicutes-Clostridia, Firmicutes-Bacilli, Tenericutes)
Firmicutes-Bacilli
Thermotoga (Firmicutes)
MreB
Actinobacteria (Acidobacteria)
Chloroflexi, Armatimonadetes
(Actinobacteria, Frimicutes)
Cyanobacteria (Aerophobetes, Firmicutes)
Spirochaetes
Elusimicrobia (Endomicrobium, Desantisbacteria)
Verrucomicrobia (Omnitrophica, Lentiphaera, Abyssubacteria)
Bacteroides, Chlorobi (Kapabacteria, Gemmatimonadetes, Persephonella, Gammaproteobacteria, Latescibacteria, Eisenbacteria, Zixibacteria, Cloacimonetes, Ignavibacteria, Edwardsbacteria, Hydrothermae, Caldiserica, Delongbacteria, Marinimicrobia)
Synergistetes (Firmicutes, Dictyoglomus, Sumerlaeota, Fibrobacteria)
Epsilonproteobacteria (Deltaproteobacteria)
Acidobacteria (Persephonella, Coatesbacteria, Chrysiogenetes, Ambiphilus, Zetaproteobacteria, Rokubacteria, Schekmanbacteria)
Nitrospirae (Methylomirabilis, Zetaproteobacteria, Deferribacteres,)
Deltaproteobacteria, Oligoflexia, Thermodesulfobacteria
(Acidobacteria, Zetaproteobacteria, Deltaproteobacteria, Alphaproteobacteria)
Betaproteobacteria, Zetaproteobacteria,
Acidithiobacillia (Gammaproteobacteria, Alphaproteobacteria)
Alphaproteobacteria
(Firmicutes, Actinobacteria, Bacteroides)
Deltaproteobacteria,Myxococcales
Firmicutes-Bacilli-Bacillales
Firmicutes-Clostridia
MreBH
Halobacteria, Izimaplasma (Spirochaetes, Firmicutes)
Spiroplasma MreB3
Spiroplasma MreB1&4
Spiroplasma MreB2&5
Firmicutes-Bacilli
(Firmicutes-Clostridia, Actinobacteria, Alphaproteobacteria)
Mbl
0.50

Figure 4

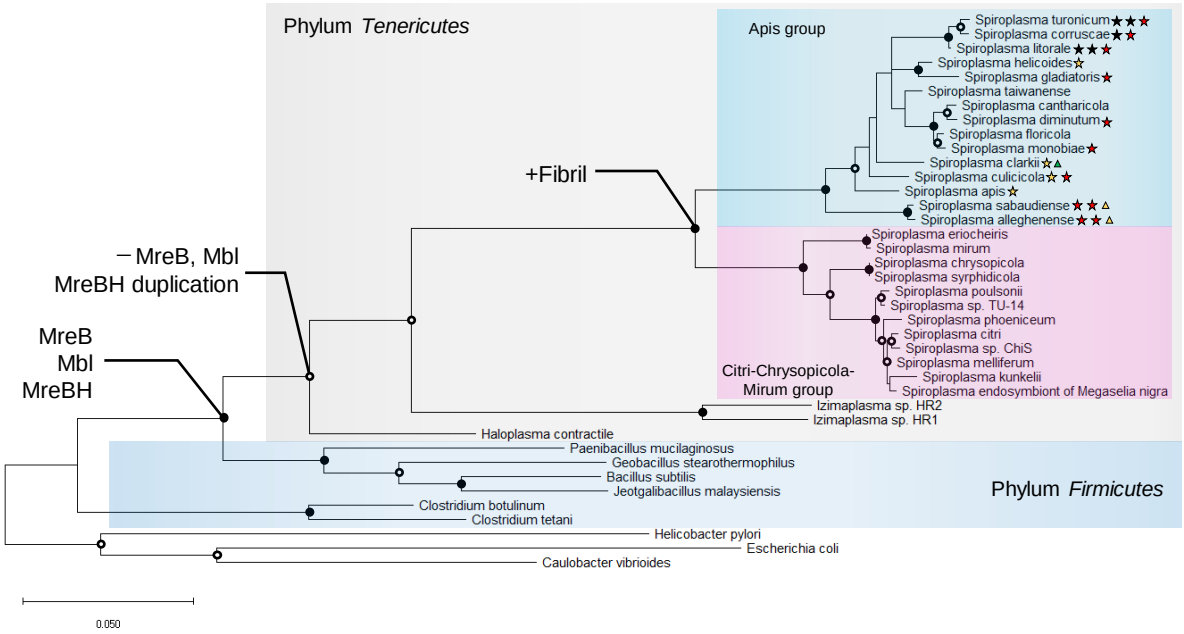
Phylum *Tenericutes*
Apis group
Spiroplasma turonicum
Spiroplasma corruscae
Spiroplasma litorale
Spiroplasma helicoides
Spiroplasma gladiatoris
Spiroplasma taiwanense
Spiroplasma cantharicola
Spiroplasma diminutum
Spiroplasma floricola
Spiroplasma monobiae
Spiroplasma clarkii
Spiroplasma culicicola
Spiroplasma apis
Spiroplasma sabaudiense
Spiroplasma alleghenense
+Fibril
−MreB, Mbl
MreBH duplication
MreB
Mbl
MreBH
Spiroplasma eriocheiris
Spiroplasma mirum
Spiroplasma chrysopicola
Spiroplasma syrphidicola
Spiroplasma poulsonii
Spiroplasma sp. TU-14
Spiroplasma phoeniceum
Spiroplasma citri
Spiroplasma sp. ChiS
Spiroplasma melliferum
Spiroplasma kunkelii
Spiroplasma endosymbiont of Megaselia nigra
Citri-Chrysopicola-
Mirum group
Izimaplasma sp. HR2
Izimaplasma sp. HR1
Haloplasma contractile
Paenibacillus mucilaginosus
Geobacillus stearothermophilus
Bacillus subtilis
Jeotgalibacillus malaysiensis
Clostridium botulinum
Clostridium tetani
Phylum *Firmicutes*
Helicobacter pylori
Escherichia coli
Caulobacter vibrioides
0.050